Adaptive Prefilter Design for Control of Quasistatic Microscanners

Klaus Janschek*, Thilo Sandner, Richard Schroedter*, Matthias Roth***

** Institute of Automation, Faculty of Electrical and Computer Engineering, Technical University Dresden, Dresden, Germany (e-mail: klaus.janschek@tu-dresden.de).*
*** Fraunhofer Institute for Photonic Microsystems (FhG-IPMS), AMS, Microscanner R&D, Dresden, Germany, (e-mail: thilo.sandner@ipms.fraunhofer.de)*

Abstract: This paper describes an open loop control approach with analog impedance feedback damping for quasistatic MEMS microscanners based on electrostatic comb transducers. The control task is determined by high dynamic input trajectory following in the presence of an extremely lightly damped mechanical mass-spring system with nonlinear electromechanical characteristics. The approach presented in this paper makes use of a model-based design approach resulting in a nonlinear adaptive prefilter for optimally preshaping of customized trajectory inputs. The open loop control is augmented by an easy to implement resistive analog impedance feedback scheme that introduces electromechanical damping and increases robustness against physical parameter uncertainties of the MEMS microscanner assembly. The paper outlines the underlying MEMS microscanner technology, it describes the mathematical model based on ANSYS computation, and it discusses in detail the proposed control concepts. Simulations and experimental results prove the applicability of the control approach.

1. INTRODUCTION

Micro Scanning Mirrors (MSM) for 1D/2D-light deflection are of particular interest for a broad range of applications as barcode reading, object identification, LIDAR, or micro displays. The advantages of small size, high-speed, low power consumption and mechanical reliability make MSMs attractive to increase the performance of existing devices and enable new fields of application, such as highly miniaturized laser projection displays. Microscanners are used in two different operating modes: resonant vs. quasistatic mode. In resonant mode, the scanner is operated at a constant frequency at or near the scanner eigenfrequency and benefits most from as low as possible viscous damping. In the *quasistatic mode*, as investigated in this paper, the extremely lightly damped mechanical mass-spring system brings up demanding operational challenges for the realization of high dynamic input trajectory (command) following.

From the mechatronics point of view, the microscanner discussed in this paper belongs to the family of electrostatic (or capacitive) transducers with comb structure. To keep the technological basis as simple as possible preferred control solutions for such transducers make use of open loop control concepts that avoid the necessity of additional displacement sensors for comb motion measurement (Borovic et al. 2005), (Ferreira and Aphale 2011). Two main obstructions for open loop control are (i) the extremely lightly damped oscillatory dynamics of an electrostatic transducer with long decay time after excitation with a control voltage and (ii) nonlinear electromechanical characteristics.

The current paper presents new contributions for overcoming above mentioned obstructions by combining *resistive (analog) impedance feedback* with *command shaping* using an *adaptive prefilter*.

The principle of *resistive impedance feedback* has been studied extensively for piezoelectric transducers, e.g. (Hagood and Flotow 1991), (Moheimani 2003), (Preumont 2006), to some extent for electrodynamic transducers, e.g. (Behrens 2005), but interestingly only rarely for electrostatic transducers, e.g. (Vargese et al. 1997). In (Janschek 2010) and (Janschek 2012) the generalization of impedance feedback has been introduced for generic reciprocal transducers and will be systematically applied for the microscanner assembly discussed in this paper.

Command or *input shaping* is a well known technique for smoothing the response of lightly damped multibody systems in macro and micro applications (Singer and Seering 1990), (Sing and Singhose 2002). The frequently used general idea is to use destructive interference of oscillatory system dynamics by applying appropriately shaped command pulses for getting minimum residual vibrations for *rest-to-rest maneuvers* (zero vibration commands). The application of such concepts for electrostatic micro-electromechanical systems (MEMS) needs extensions for taking into account their inherent nonlinearities in particular for variable plate distance arrangements (pull in phenomenon), e.g. (Chen and Ou 2007), (Ou et al. 2011). Another smart technique for shaping of *linear velocity commands* has been proposed by (Schitter et al. 2008) where the edges of a triangular command profiles are cut and kept at constant displacement for half the period of the eigenmode and thus implying the destructive interference principle. A powerful approach that has become popular in the last decade is the flatness-based trajectory generation, and it has been applied also successfully to electrostatic transducers, e.g. (Zhu et al. 2006). All these approaches result in general in pre-computed (offline) trajectories that can be stored easily in look-up

Post-print version of the article: K. Janschek, T. Sandner, R. Schroedter, M. Roth, "Adaptive Prefilter Design for Control of Quasistatic Microscanners", *Proc. of 6th IFAC Symposium on Mechatronic Systems*, vol. 46 (5), pp. 197-206, 2013.
DOI: 10.3182/20130410-3-CN-2034.00112

tables, but that cannot be modified easily for changing (online) characteristics.

The most straightforward approach for minimization of vibration residuals is the remove critical excitation frequencies from the input command spectrum, resulting in prefiltering schemes using the inverse system dynamics e.g. (Milanović and Castelino 2004), (Zeitz 2012). The advantages of inverse prefiltering in terms of easy implementation and independence of the actual command profile are being lost, however, in many real world applications by its sensitivity to model uncertainties in particular to eigenfrequency variations for lightly damped eigenmodes.

The current paper shows how the inverse prefiltering scheme can nevertheless be applied in a robust manner for open loop control of quasistatic microscanners. The proposed concept combines resistive analog impedance feedback and a nonlinear command shaping prefilter with notch characteristics, which is adaptive to mirror deflections. The electromechanical damping introduced by simple and easy to implement means of analog impedance feedback will gain robustness against eigenfrequency uncertainties and thus allowing an efficient and robust use of even constant prefilter variants.

The paper is arranged as follows: Sect. 2 introduces the used microscanner technology and specifies the key system requirements for dynamic operation. Sect. 3 presents the model basis used for deriving the model-based control concepts, in Sects. 4 and 5 the two key concepts impedance feedback and adaptive prefilter are introduced and demonstrated by simulation experiments, an experimental validation of these concepts with real world experiments is presented in Sect. 6.

2. MICROSCANNER LAYOUT AND OPERATIONAL REQUIREMENTS

One of the most recognized MEMS scanner devices is the electrostatically and resonantly driven MSM of the Fraunhofer Institute for Photonic Microsystems - IPMS (Schenk et al. 2009) that are proven for reliable industrial fabrication. However, these 2D MSMs with in-plane vertical comb drives are limited to resonant operation at a fixed frequency or frequency ratio. Thus, the scan trajectory is fixed and depends on the amplitude and the frequency ratio predefined by the MEMS design.

Recently, IPMS extended its scanner technology to quasistatic actuation using three-dimensional vertical out-of–plane comb drives. In Fig. 1, the basic configuration of a quasistatic microscanner is shown for a staggered vertical comb (SVC) drive – where the movable, and fixed driving electrodes are out-of-plane shifted for rest position of the spring suspended scanning mirror. The driving voltages (U1, U2) are applied separately to the two fixed driving electrodes, whereas the movable electrode is connected to the ground, enabling quasistatic forward and backward actuation of the scanning mirror. The scanning mirror consists of a high Q spring mass system only very lowly damped by the surrounding viscous gas.

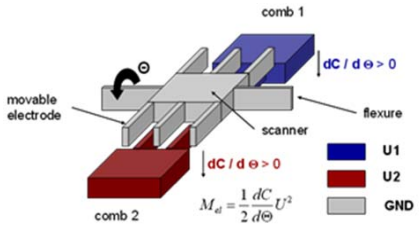

Fig. 1. Schematic configuration of quasistatic microscanner with staggered vertical comb (SVC) drive

The novel device concept of IPMS for vertical 3D comb drives is realized as a system-in-package device and assembly (Sandner et al. 2011). The geometry of the vertical comb is dependent on the solid body mechanism used to deflect the fixed electrode from the in plane fabrication position to the desired out of plane position (Jung et al. 2012). Depending on the design of solid body mechanism both staggered (SVC) or more efficient angular (AVC) comb drives can be realized within the same process. In contrast to state of the art for MSM with 3D comb drives (Milanović et al. 2002), (Piyawattanametha et al. 2005) the IPMS approach enables larger scan angles up to ±10° combined with simplified and reliable fabrication with high flexibility of drive geometry only by design without technological changes. The technology approach is reported in more detail in (Jung et al. 2009).

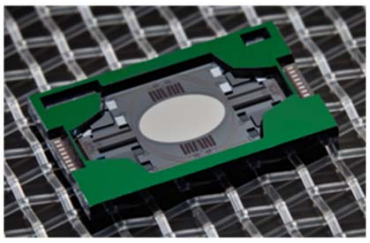

Fig. 2. Photograph of quasistatic / resonant 2D-Microscanner developed by FhG-IPMS

The gimbal suspended quasistatic / resonant 2D-MEMS scanning mirrors reported in this article (cf. Fig. 2) have been developed in particular for the novel concept of an adaptive 3D TOF laser camera with foveation properties (Thielemann et al. 2010) to allow e.g. future autonomous robots to better interact with their surroundings. The sensor concept of foveation – that is acquiring distance images with coarse spatial resolution, rapidly detecting regions of interest (ROI), and then concentrating further image acquisition on these ROIs with adaptive scanning – requires a challenging 2D scanning device with quasi-static actuation, large effective aperture ≥ 5mm and > 60° FOV. The best technical compromise of the fast adaptive scanning unit were found in a synchronized driving of multiple raster scanning MEMS mirrors to meet opposite requirements of fast scanning (> 1000Hz), large scan range and large effective aperture. Therefore, IPMS developed a quasi-static resonant MEMS raster scanning mirror (Fig. 2), where SVC comb drives enables quasi-static mechanical deflections of ±10°. Resonant

Post-print version of the article: K. Janschek, T. Sandner, R. Schroedter, M. Roth, "Adaptive Prefilter Design for Control of Quasistatic Microscanners", *Proc. of 6th IFAC Symposium on Mechatronic Systems*, vol. 46 (5), pp. 197-206, 2013.
DOI: 10.3182/20130410-3-CN-2034.00112

For further information contact: schroedter@acin.tuwien.ac.at, https://orcid.org/0000-0003-3259-4571

horizontal scanning at 1600Hz guarantees a large optical scan range up to 80° even for a 2.6x3.6mm single mirror. To provide the full 5mm effective reception aperture of the TOF camera, five hybrid assembled MEMS mirrors are precisely synchronized with respect to the sending mirror of the TOF laser scanner. For prospective real-time feedback control, piezo-resistive position sensors are integrated on chip for both scanning axis, but not taken into account for the open loop control approach investigated in the current paper. The novel 3D TOF camera provides a distance measuring rate of 1MVoxel/s and an uncertainty of TOF distance measurement of 3mm at 7.5m measuring range enabling e.g. 3D images with 1Mpixel per second or 100Kpixel frames per second, respectively, over a 40°x60° (potentially 60°x80°) FOV.

The main application requirement for the design presented in this paper defines the *scan trajectory* of the quasistatic vertical scan axis providing a linearized scanning below scanner eigenfrequency of 125Hz. Typically are required (i) symmetric triangular scanning patterns at 10Hz or (ii) symmetric linear scan patterns with reduced scanning velocity for higher resolved TOF measurement in ROI's. To achieve the full effective reception aperture of the adaptive 3D TOF camera the maximum deviation of temporal angular scan position is limited to 0.1° for all five scanning mirrors over the entire scan range due to the small FOV of the fibre coupled detector optics.

3. PHYSICAL MODELING

The microscanner assembly represents a reciprocal electrostatic transducer, and the further modeling follows the generic mechatronic transducer approach according to (Janschek 2012). A conceptual model of the microscanner is given in Fig. 3. The movable comb with attached micromirror (inertia J_M, deflection q) is suspended above the substrate via a torsional spring with deflection dependent torsional stiffness $k(q)$ and linear mechanical damping b. Linear mechanical damping originates from the mirror plate moving in air (fluid damping) and attains only very small values. Open loop control approaches derived in this paper will thus neglect the fluid damping and focus on damping originating from impedance feedback, specifically a resistor R connected in series to the voltage controlled power amplifier with output voltage $u_S(u_{ref})$. The input reference voltage u_{ref} represents the control input to the microscanner.

Figure 4 depicts the (differential) stiffness of the torsional spring as a function of the deflection q of the mirror plate (ANSYS model). The spring suspension shows a progressive behavior with stiffening more than 30% at increasing deflection. The nonlinear spring suspension torque is given by

$$\tau_{spring}(q) = \int_0^q k(q')dq' \,. \tag{1}$$

The driving torque τ_{el} of the comb drive actuator is given by

$$\tau_{el}(q, u_D) = \frac{1}{2}\frac{\partial C(q)}{\partial q} u_D^2 \tag{2}$$

with the deflection dependent capacitance function $C(q)$ and the drive voltage u_D. Eq. (2) shows the well known unidirectional behavior, where the movable comb is attracted by the static comb for increasing the capacitance. As a consequence, a second comb drive is needed allowing bipolar mirror deflections (cf. Fig. 1). Figure 5 shows the corresponding capacitance as a function of the deflection (ANSYS model). The derivative with respect to the deflection resolves to be nearly constant.

Rotational inertia was found to be $J_M = 4.35 \cdot 10^{-12}\,\mathrm{kgm}^2$ while the mechanical damping coefficient is $b = 3.3 \cdot 10^{-11}\,\mathrm{Nms/rad}$. The input voltage u_D was restricted to $\pm 150\,V$.

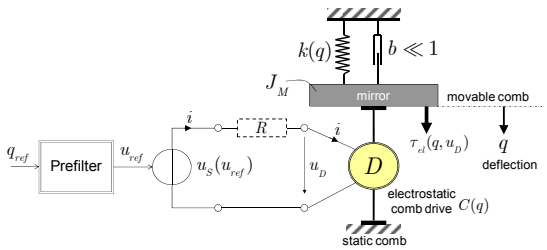

Fig. 3. Conceptual model of the microscanner: electrostatic comb drive with a micromirror mounted on top of an elastically suspended movable comb

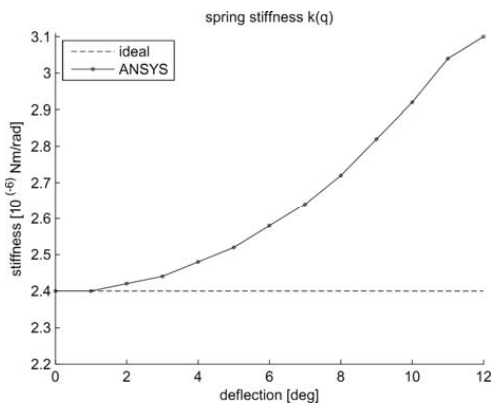

Fig. 4. Stiffness function $k(q)$: ANSYS characteristic (negative deflection mirrored)

Post-print version of the article: K. Janschek, T. Sandner, R. Schroedter, M. Roth, "Adaptive Prefilter Design for Control of Quasistatic Microscanners", *Proc. of 6th IFAC Symposium on Mechatronic Systems*, vol. 46 (5), pp. 197-206, 2013.
DOI: 10.3182/20130410-3-CN-2034.00112

For further information contact: schroedter@acin.tuwien.ac.at, https://orcid.org/0000-0003-3259-4571

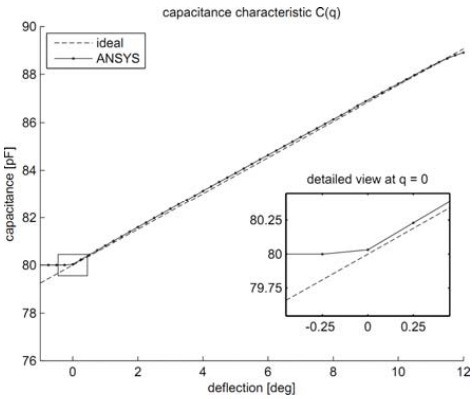

Fig. 5. Capacitance function $C(q)$: general structure for positive deflection (negative deflection mirrored), ANSYS characteristic

The nonlinear dynamic microscanner model takes into account the nonlinear mechanical and transducer torques Eqs. (1), (2) as well as the nonlinear electromechanical coupling

$$\begin{aligned} J_M\,\ddot{q} + b\,\dot{q} + \tau_{spring}(q) &= \tau_{el}(q, u_D) \\ i(q, \dot{q}, u_D, \dot{u}_D) &= C(q)\,\dot{u}_D + \frac{\partial C(q)}{\partial q}\,\dot{q}\,u_D \end{aligned} \quad . \tag{3}$$

The local linearization of Eq. (3) at an operating point $(q_0, u_{D,0})$ with $\Delta q = q - q_0$, $\Delta u_D = u_D - u_{D,0}$ leads to a linear small signal dynamic model as depicted in Fig. 6 with the model parameters (cf. (Janschek 2012))

$$\begin{aligned} k_{el} &:= \frac{\partial C^2(q)}{\partial q^2}\,u_D^2\Big|_{\substack{u_D = u_{D,0} \\ q = q_0}}, \quad K_{el} := \frac{\partial C(q)}{\partial q}\,u_D\Big|_{\substack{u_D = u_{D,0} \\ q = q_0}}, \\ C_R &:= C(q)\big|_{q = q_0}, \qquad k_R := k(q)\big|_{q = q_0} . \end{aligned} \tag{4}$$

The block diagram model in Fig. 6 shows transparently the reciprocal transducer behavior via the mutual electro-mechanical coupling K_{el}. For design purposes, the two transfer functions between drive voltage Δu_D and deflection Δq (mechanical response) resp. drive current Δi (electrical response) are of further interest

$$\begin{aligned} G_{q/u}(s) &= \frac{\Delta Q(s)}{\Delta U_D(s)} = V_{q/u}\,\frac{1}{\{d_0, \Omega_U\}} \\ G_{i/u}(s) &= \frac{\Delta I(s)}{\Delta U_D(s)} = V_{i/u}\,\frac{s\{d_0, \Omega_I\}}{\{d_0, \Omega_U\}} \end{aligned} \tag{5}$$

with parameters

$$\begin{aligned} k_D &:= k_R - k_{el}, \quad V_{q/u} := \frac{K_{el}}{k_D}, \quad V_{i/u} := C_R\,\frac{k_R}{k_D}, \\ \Omega_U^{\,2} &:= \frac{k_D}{J_M}, \quad \Omega_I^{\,2} := \frac{k_D + K_{el}^{\,2}/C_R}{J_M}, \quad d_0 \approx 0 , \end{aligned} \tag{6}$$

and polynomial symbolic abbreviations

$$\{d_i, \Omega_i\} := 1 + 2d_i\,\frac{s}{\Omega_i} + \frac{s^2}{\Omega_i^2} \quad , \quad [\omega_i] := 1 + \frac{s}{\omega_i} . \tag{7}$$

Due to the very low mechanical damping $b \ll 1$ the microscanner represents a very lightly damped oscillator with the eigenfrequency $f_U \approx 125$ Hz $(\Omega_U = 2\pi f_U)$. All transfer function parameters are varying according to the operating point $(q_0, u_{D,0})$. For a more detailed physical interpretation of the parameters in Eq. (6) see (Janschek 2012).

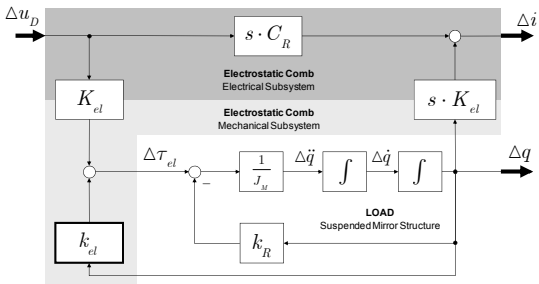

Fig. 6. Small signal linear model of the electrostatic comb drive with voltage control

4. RESISTIVE IMPEDANCE FEEDBACK

The poorly damped oscillatory dynamics of the micromirror according to Eq. (5) is prohibiting efficient open loop control concepts due to the low damped oscillations and long decay time after excitation with a control input voltage. Instead of increasing the mechanical damping (which is moreover difficult from the technological point of view) a much smarter mechatronic concept is to use the transducer's reciprocal power properties by implementing a so called resistive impedance feedback. The approach used hereafter follows the generic representation introduced by (Janschek 2010), (Janschek 2012).

For a resistive *impedance* R in *series* with the power amplifier output port according to Fig. 3 the KIRCHHOFF loop law shows

$$u_D = u_S - R \cdot i \ . \tag{8}$$

The signal flow interpretation of Eq. (8) reveals an electrical *analog feedback* of the transducer current Δi via the impedance R as sketched in Fig. 7.

Post-print version of the article: K. Janschek, T. Sandner, R. Schroedter, M. Roth, "Adaptive Prefilter Design for Control of Quasistatic Microscanners", *Proc. of 6th IFAC Symposium on Mechatronic Systems*, vol. 46 (5), pp. 197-206, 2013.
DOI: 10.3182/20130410-3-CN-2034.00112

For further information contact: schroedter@acin.tuwien.ac.at, https://orcid.org/0000-0003-3259-4571

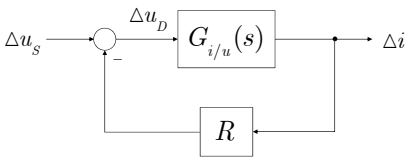

Fig. 7. Impedance feedback: block diagram model

From the control loop representation in Fig. 7, it follows that the poles of the closed loop dynamics can easily be constructed graphically from the standard *root locus* with $G_{i/u}(s)$ as open loop (plant) transfer function. Taking into account the pole-zero configuration of $G_{i/u}(s)$ from Eqs. (5), (6), i.e. imaginary poles and zeroes at $\pm j\Omega_U, \pm j\Omega_I$ and $\Omega_U < \Omega_I$, the respective root loci are shown in Fig. 8.

The impedance feedback results in the following fundamental properties for the microscanner dynamics (Janschek 2010): (i) resistive feedback introduces one additional (stable) real pole to the microscanner dynamics, (ii) resistive feedback introduces damping for the microscanner eigenfrequency, even if the mechanical damping b is zero, (iii) the maximum feedback damping does not occur at maximum resistance, but at some intermediate value. The optimal values for feedback damping and resistance can be found as, see (Janschek 2012), (Preumont 2006)

$$\tilde{d}_U^{\max} = \frac{|\Omega_U - \Omega_I|}{2\min(\Omega_U, \Omega_I)}, \tag{9}$$

$$R^{opt} = \frac{1}{C_R}\frac{1}{\Omega_I}\sqrt{\frac{\Omega_U}{\Omega_I}} \quad . \tag{10}$$

The most interesting results of introducing resistive impedance feedback are that (i) the resistor R introduces a simple and easy way for implement analog electromechanical damping and (ii) a careful selection of the series resistor in Fig. 3 offers an important and efficient design degree of freedom.

The microscanner under consideration shows an inherent resistance at the electrical port of $R_0 = 1\ \mathrm{k\Omega}$, whereas the optimal impedance according to Eq. (10) at linearization point $q_0 = 4°$ is about $R^{opt} = 15\ \mathrm{M\Omega}$.

The dissipative effect for different values of R and consequences resulting on the mechanical transient dynamics are shown in Fig. 9 for a step input u_{ref} (cf. Fig. 3). The decay time for the eigenfrequency oscillation is minimal indeed for $R^{opt} = 15\ \mathrm{M\Omega}$. A larger resistance decreases the oscillation amplitude, but also decreases the damping and hence increases the decay time, moreover it introduces also a larger first order time lag (real pole $p_2 \rightarrow p_3$, Fig. 9).

Thus, a simple design modification of the electrical port of the microscanner by adding a series resistor changes considerably the dynamic properties and opens advantageous potentials for easy to implement open loop control concepts for dynamic microscanner operation.

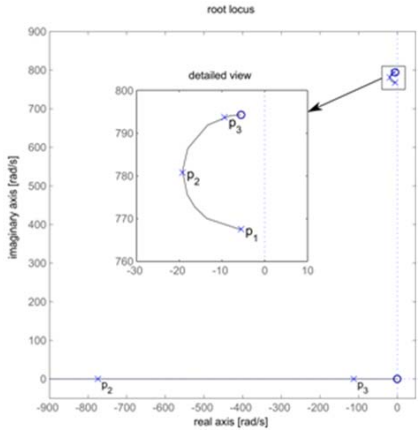

Fig. 8. Root locus (upper half complex plane) for impedance feedback with closed loop poles p_1 @ $R = 1\ \mathrm{k\Omega}$, p_2 @ $R = 15\ \mathrm{M\Omega}$ and p_3 @ $R = 100\ \mathrm{M\Omega}$

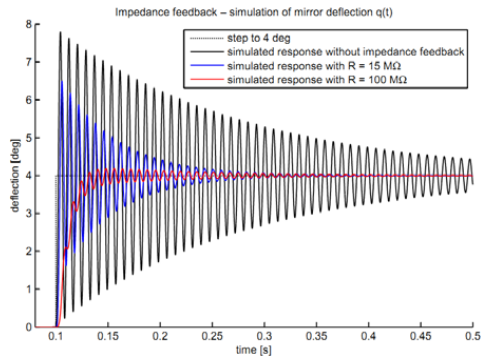

Fig. 9. Impedance feedback – mirror deflection $q(t)$: simulated step response for different resistive impedances (nonlinear microscanner model Eq. (3), *with* static gain adaptation, *without* dynamic prefilter, cf. Fig. 10)

5. ADAPTIVE PREFILTER

5.1 Microscanner Design Model

A well known open loop control concept is command shaping by dynamically prefiltering the reference commands based on a sufficiently representative model of the system to be controlled (here: microscanner). The type of model always has to be adapted to the type and dynamic properties of the reference commands. In the current microscanner application, typical reference commands comprise triangular scan patterns well below the scanner eigenfrequency (cf. Sect. 2).

One interesting candidate design model, which takes into account the nonlinear deflection characteristics, is given by a combination of the linearized model Eq. (5) jointly with the variable (i.e. deflection dependent) electromechanical parameters of Eq. (4). This model is called further on the

Post-print version of the article: K. Janschek, T. Sandner, R. Schroedter, M. Roth, "Adaptive Prefilter Design for Control of Quasistatic Microscanners", *Proc. of 6th IFAC Symposium on Mechatronic Systems*, vol. 46 (5), pp. 197-206, 2013.
DOI: 10.3182/20130410-3-CN-2034.00112

For further information contact: schroedter@acin.tuwien.ac.at, https://orcid.org/0000-0003-3259-4571

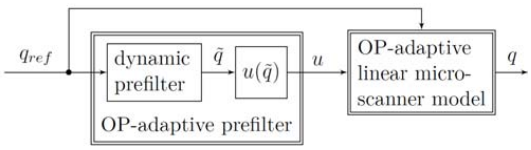

Fig. 10. Design model for the operating point OP-adaptive prefilter

operating point (OP-) adaptive linear microscanner model (cf. Fig. 10). Due to the rather low frequency band of reference commands there exists a sufficient decoupling of microscanner dynamics (eigenfrequency $f_U \approx 125$ Hz) and reference signal dynamics (typ. $f_{ref} = 10$ Hz). In such a case a deflection based adaptation of the small signal model parameters Eq. (6) promises a representative modeling of the deflection dependent change of microscanner dynamics.

For the prefilter design, the following *OP-adaptive linear microscanner model* is used when *no impedance feedback* is applied (compare Eqs. (4) to (6)):

$$G_0(s, q_{ref}) = \frac{V(q_{ref})}{\left\{d_0(q_{ref}), \Omega_0(q_{ref})\right\}},$$
$$V(q_{ref}) = \frac{K_{el}(q_{ref})}{k\left(q_{ref}\right) - k_{el}(q_{ref})},$$
$$\Omega_0(q_{ref}) = \sqrt{\frac{k(q_{ref}) - k_{el}(q_{ref})}{J_M}}, \tag{11}$$
$$d_0(q_{ref}) = \frac{1}{2}\frac{b}{k(q_{ref}) - k_{el}(q_{ref})}\sqrt{\frac{k(q_{ref}) - k_{el}(q_{ref})}{J_M}}.$$

The dependency of the transfer function parameters in Eq. (11) from the mirror deflection q_{ref} is sketched in Fig. 11 (shaded area specifies the considered operating range).

For *impedance feedback,* the *OP-adaptive linear micro-scanner model* has the extended form

$$G_R(s, q_{ref}) = \frac{V(q_{ref})}{\left\{d_R(q_{ref}), \Omega_R(q_{ref})\right\}\left[\omega_R(q_{ref})\right]} \tag{12}$$

where the parameters d_R, Ω_R, ω_R can be computed easily taking into account the feedback structure in Fig. 7 (cf. abbreviations for linear and quadratic terms according to Eq. (7)).

5.2 Command Shaping Prefilter

The block diagram representation of the command shaping prefilter as sketched in Fig. 10 fulfils two correcting purposes: (i) dynamic shaping of reference deflections q_{ref} (left block), and (ii) static gain adaptation (right block).

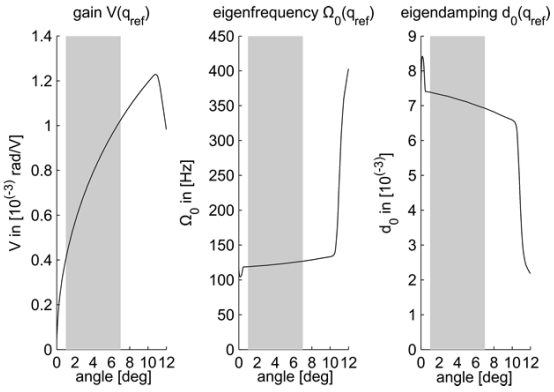

Fig. 11. OP-adaptive linear microscanner model: gain, eigenfrequency and eigendamping as a function of the operating point (OP) q_{ref}; operating angle range (1° to 7°) with gray colour

The *static gain adaption* law (*static prefilter*) is defined by (cf. Eqs. (1) to (3))

$$u_{ref}(\tilde{q}) = \sqrt{\frac{\int_0^{\tilde{q}} k(q)dq}{\frac{1}{2}\frac{\partial C(\tilde{q})}{\partial \tilde{q}}}} \tag{13}$$

that assures a proper adaptation of the input voltage command u_{ref} of the microscanner (cf. Fig. 3).

For *dynamic shaping* of the reference deflection commands a compensating filter – *dynamic prefilter* (cf. Fig. 11) – with notch characteristic is proposed, i.e.

– dynamic prefilter *without* impedance feedback (cf. Eq. (11))

$$P_0(s, q_{ref}) = \frac{\left\{d_R(q_{ref}), \Omega_R(q_{ref})\right\}}{\left\{d_p, \Omega_p\right\}}, \tag{14}$$

– dynamic prefilter *with* impedance feedback (cf. Eq. 12)

$$P_0(s, q_{ref}) = \frac{\left\{d_R(q_{ref}), \Omega_R(q_{ref})\right\}\left[\omega_R(q_{ref})\right]}{\left\{d_p, \Omega_p\right\}\left[\omega_p\right]}. \tag{15}$$

The filter poles in Eqs. (14), (15) have to be selected taking into account the limitation of the control voltage u_{ref} of the microscanner (the larger the magnitude of the poles, the larger the output amplitudes of the prefilter due to differentiating behaviour).

Typical operational performances and performance improvements for impedance feedback and prefilter use can be seen from simulation results presented in Figs. 12 and 13 with prefilter parameters listed in Table 1. The simulations have been performed with the full nonlinear model Eq. (3) and they are therefore fully representative for the microscanner configuration in Fig. 3. As expected, both

Post-print version of the article: K. Janschek, T. Sandner, R. Schroedter, M. Roth, "Adaptive Prefilter Design for Control of Quasistatic Microscanners", *Proc. of 6th IFAC Symposium on Mechatronic Systems*, vol. 46 (5), pp. 197-206, 2013.
DOI: 10.3182/20130410-3-CN-2034.00112

For further information contact: schroedter@acin.tuwien.ac.at, https://orcid.org/0000-0003-3259-4571

impedance feedback and model based command shaping improve the tracking performance considerably.

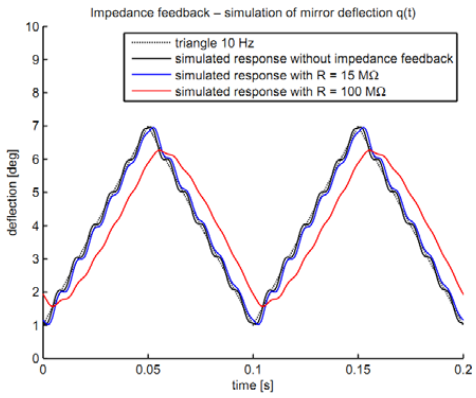

Fig. 12. Impedance feedback – mirror deflection $q(t)$: simulated triangle response with 10 Hz between 1° and 7° (nonlinear microscanner model Eq. (3), *with* static gain adaptation, *without* dynamic prefilter, cf. Fig. 10)

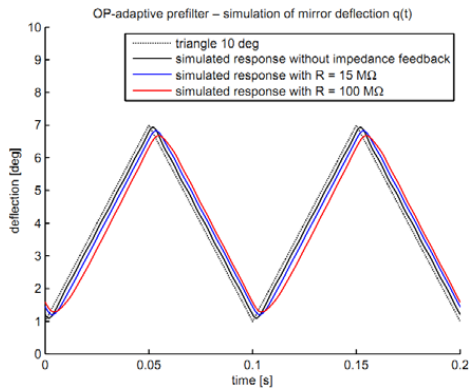

Fig. 13. OP-adaptive prefilter: simulation result of mirror deflection $q(t)$ for characteristic input trajectory with impedance feedback

Table 1. Prefilter coefficients using eigenfrequency $\Omega_0 = 123.8$ Hz at linearization point $q_0 = 4°$

	R = 1 kΩ	R = 15 MΩ	R = 100 MΩ
d_p	0.7	1	2
Ω_p	Ω_0	Ω_0	Ω_0
ω_p	-	Ω_0	Ω_0

6. EXPERIMENTAL RESULTS

6.1 Experiment Setup

The experimental verification of the proposed open loop control concept aims at (i) validation of microscanner model accuracy and (ii) performance assessment under operational conditions. The experiments have been conducted with a FhG-IPMS developed microscanner according to Fig. 2 in a test setup shown in Fig. 14. External reference measurement of the real mirror deflection $q(t)$ has been performed with a position sensitive detector (PSD) setup as sketched in Fig. 15.

The measurement equation for mirror angle $q(t)$ using the PSD is given as

$$\hat{q} = \frac{1}{2}\arcsin\left(\frac{k_{PSD}}{d}\frac{I_a - I_b}{I_a + I_b}\right)$$

where I_a, I_b are displacement currents, d the distance between PSD and micro mirror and k_{PSD} is a scaling factor.

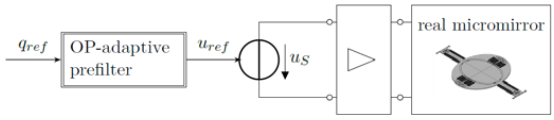

Fig. 14. Experimental setup with OP-adaptive prefilter

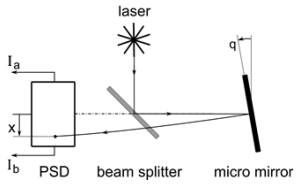

Fig. 15. Experimental setup for measurement of mirror deflection $q(t)$

6.2 Microscanner Model Validation

The model based design approach as presented in Sect. 5 relies fundamentally on a representative model of the microscanner arrangement and thus needs a careful validation of the model accuracy. The experimental results for step commands are given in Fig. 16 and comparing them with the equivalent simulations given in Fig. 9 shows a very good coincidence. Thus, the baseline model Eq. (3) including the parameters as given in Sect. 3 proves to be highly representative.

6.3 Microscanner Operational Performance Results

The operational performances of the microscanner have to be assessed for triangular deflection reference commands as specified in Sect. 2. A series of experiments has been performed with deflection reference commands, equivalent to those given in Figs. 12 and 13.

A summary of performance metrics based on statistical evaluation is given in Tables 2 and 3 with

Post-print version of the article: K. Janschek, T. Sandner, R. Schroedter, M. Roth, "Adaptive Prefilter Design for Control of Quasistatic Microscanners", *Proc. of 6th IFAC Symposium on Mechatronic Systems*, vol. 46 (5), pp. 197-206, 2013.
DOI: 10.3182/20130410-3-CN-2034.00112

For further information contact: schroedter@acin.tuwien.ac.at, https://orcid.org/0000-0003-3259-4571

$$e_{q,\max}(t_i) = \max_{100\ \text{cycles}} \left| q_{ref}(t_i) - \hat{q}(t_i) \right| \ , \tag{16}$$

$$\Delta\overline{q}(t_i) = \max_{100\ \text{cycles}} \left| \hat{q}(t_i) - \operatorname{mean}_{100\ \text{cycles}}(\hat{q}(t_i)) \right| \ , \tag{17}$$

$$\Delta\overline{q}_{\max} = \max_{t_i} \left(\Delta\overline{q}(t_i) \right) \ , \tag{18}$$

$$\Delta\overline{\sigma} = \operatorname{std}_{t_i} \left(\hat{q}(t_i) - \operatorname{mean}_{100\ \text{cycles}}(\hat{q}(t_i)) \right). \tag{19}$$

The maximum tracking error is represented by Eq. (16), whereas Eqs. (17) to (19) represent metrics for repeatability of successive scans evaluated for 99 triangle cycles.

Time behavior metrics are given in Fig. 17 with cross reference to relevant metrics according to Eqs. (16) to (19).

6.4 Performance Assessment and Design Evaluation

First of all it can be stated that the experimental results prove the feasibility of the proposed model based open loop microscanner control concept under real world conditions.

Repeatability – A high repeatability of successive scans scanning needs a smooth, linear increasing/decreasing trajectory (cf. Fig. 17 area II). The results of Table 2 and Fig. 17c,d show clearly the positive effect of *impedance feedback* in smoothing the mirror oscillations. Although a bigger resistance smoothens better, the optimal resistor $R^{opt} = 15\text{M}\Omega$ according to Eq. (10) introduces considerably less phase lag and should be preferred.

Tracking error – The specification requires maximum deviation of temporal angular scan position less than 0.1° (cf. Sect. 2). The results of Table 3 and Fig. 17b show clearly the positive effect of a dynamic prefilter. Interestingly even a *constant prefilter* already meets the requirements and the further improvement with a full adaptive dynamic prefilter is not more than 20 percent.

Design conclusions – The proposed design approach offers three design degrees of freedom (i) *resistive impedance* R, (ii) *static prefilter* and (iii) *dynamic prefilter* (constant vs. adaptive), with all three needed to meet the performance requirements. For the current application, even a very *simple* fully *analog* realization (on-chip) for all three elements can be envisaged. The dynamic prefilter could be implemented as a linear filter with constant parameters, which will result only in a slight performance degradation w.r.t. the OP-adaptive variant.

Table 2. Experimental results: Repeatability for different impedance feedback without dynamic prefilter (configuration: static prefilter; statistics from 99 triangle cycles; see Fig. 17c,d)

	$\Delta\overline{q}_{\max}$	$\Delta\overline{\sigma}$
no impedance feedback	0.0453°	0.0211°
R = 15 MΩ	0.0165°	0.0093°
R = 100 MΩ	0.0105°	0.0056°

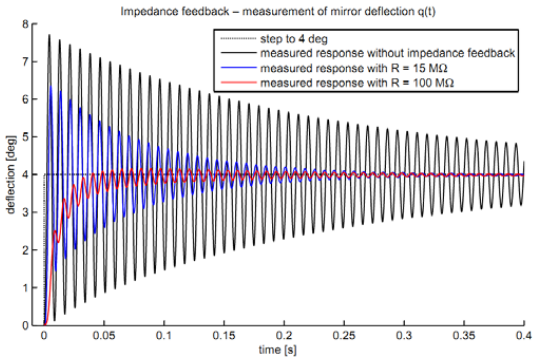

Fig. 16. Experimental results of mirror deflection $q(t)$ for step commands and resistive impedance feedback (*with* static gain adaptation, *without* dynamic prefilter, cf. Fig. 10)

Table 3. Experimental results: Maximum tracking errors for different dynamic prefilter variants (configuration: *static prefilter* and *impedance feedback* @ R=15MΩ; area I/II see Fig. 17b)

	$e_{q,\max}$ area I	$e_{q,\max}$ area II
no dynamic prefilter (cf. Fig. 17b)	0.2085	0.2407
constant dynamic prefilter at 4°	0.2460	0.0840
full OP-adaptive prefilter	0.2190	0.0705

7. CONCLUSIONS

This paper has shown a combination of resistive impedance feedback and command shaping adaptive prefilter for robust open loop control of a quasistatic micromirror. Experimental results have proved that linear scan patterns with high reproducibility can be realized with rather simple means. An important result of this work is also the successful experimental validation of the mathematical model of the microscanner. The good quality of the micromirror model offers the possibility for different promising design improvements. A systematic minimization of performance metrics like those presented in Sect. 6 can efficiently be performed by computer-based optimization of the design degrees of freedom (resistor, prefilter parameters) based on the representative and now validated simulation model, cf. (Janschek 2012). A different path for current research is dealing with nonlinear model based trajectory generation for the full bidirectional deflection range, i.e. positive to negative with zero crossing (Schroedter et al. 2013) and model based self-calibration of the prefilter parameters.

REFERENCES

Behrens, S., Fleming, A. J., Moheimani, S. O. R. (2005) Passive vibration control via electromagnetic shunt damping. Mechatronics, IEEE/ASME Transactions on 10(1): 118-122

Borovic, B., Hong, C., Zhang, X.M., Liu, A.Q., Lewis, F.L. (2005) Open vs. Closed-Loop Control of the MEMS Electrostatic

Post-print version of the article: K. Janschek, T. Sandner, R. Schroedter, M. Roth, "Adaptive Prefilter Design for Control of Quasistatic Microscanners", *Proc. of 6th IFAC Symposium on Mechatronic Systems*, vol. 46 (5), pp. 197-206, 2013.
DOI: 10.3182/20130410-3-CN-2034.00112

For further information contact: schroedter@acin.tuwien.ac.at, https://orcid.org/0000-0003-3259-4571

Comb Drive, In: Proceedings of the 2005 IEEE International Mediterrean Conference on Control and Automation, pp. 982 – 988.

Chen, K.-S., Ou, K.-S. (2007) Command-Shaping Techniques for Electrostatic MEMS Actuation: Analysis and Simulation, Journal of Microelectromechanical Systems, Volume 16 , Issue 3, pp.537-549.

Ferreira, A., Aphale, S.S. (2011) A Survey of Modeling and Control Techniques for Micro- and Nanoelectromechanical Systems, IEEE Transactions on Systems, Man, and Cybernetics—Part C: Applications and Reviews, Vol. 41, No. 3, pp. 350-364.

Hagood, N. W., Flotow, A. v. (1991) Damping of structural vibrations with piezoelectric materials and passive electrical networks. Journal of Sound and Vibration 146(2): 243-268

Janschek, K. (2010) The Generic Mechatronic Transducer Model – A Unified System Modeling Approach. In: *Proceedings of 5th IFAC Symposium on Mechatronic Systems, September 13-15, 2010, Cambridge, MA, USA* (IFAC-PapersOnLine, ID 10.3182/20100913-3-US-2015.00060), pp. 267-276.

Janschek, K. (2012) *Mechatronic Systems Design: Methods, Models, Concepts*. Springer.

Jung, D., Sandner, T., Kallweit, D., Schenk, H. (2012) Vertical comb drive microscanners for beam steering, linear scanning, and laser projection applications. In: Proc. SPIE 8252, MOEMS and Miniaturized Systems XI, 82520U (February 9, 2012); doi:10.1117/12.906690.

Jung, D. et al. (2009) Fabrication of 3D Comb Drive Microscanners by mechanically induced permanent Displacement, In: Proc. of SPIE 7208, pp. 72080A-1--11, San Jose, USA.

Milanović, V. et al. (2002) Monolithic vertical combdrive actuators, Proc. IEEE/LEOS Conf. Optical MEMS, pp. 57-58.

Milanović, V., Castelino, K. (2004) Sub-100 µs Settling Time and Low Voltage Operation for Gimbal-less Two-Axis Scanners, IEEE/LEOS Optical MEMS 2004, Takamatsu, Japan, Aug. 2004.

Moheimani, S. O. R. (2003) A survey of recent innovations in vibration damping and control using shunted piezoelectric transducers. IEEE Trans. Control Systems Technology, 11(4): 482-494.

Ou, K.-S., Chen, K.-S., Yang, T.-S., Lee, S.-Y. (2011) Fast Positioning and Impact Minimizing of MEMS Devices by Suppression of Motion-Induced Vibration by Command-Shaping Method, Journal of Microelectromechanical Systems, Vol. 20, No.1, pp. 128 –139.

Piyawattanametha, W. et al. (2005) Surface- and Bulk-Micromachined Two-Dimensional Scanner Driven by Angular Vertical Comb Actuators, J. of MEMS, Vol. 14, No. 6 pp. 1329-1338.

Preumont, A. (2006) Mechatronics, Dynamics of Electromechanical and Piezoelectric Systems, Springer

Sandner, T., Jung, D., Kallweit, D., Grasshoff, T., Schenk, H. (2011) Microscanner with Vertical out of Plane Combdrive, *IEEE/LEOS Proc. Int. Conf. on Optical MEMS & Nanophotonics, 2011.*

Schenk, H., Sandner, T. et al.: Single crystal silicon micro mirrors, Phys. Status Solidi C, (2009), pp. 1– 8.

Schitter, G., Thurner, Ph.J., Hansma, P.K. (2008) Design and input-shaping control of a novel scanner for high-speed atomic force microscopy, Mechatronics, Volume 18, Issues 5–6, June 2008, pp. 282-288.

Schroedter, R., Roth, M., Sandner, T., Janschek, K. (2013) Model-based motion tracking for quasistatic microscanners (in German). In: Proceedings of the Fachtagung Mechatronik 2013, 6.-8.3.2013, Aachen, Germany, ISBN3-86130-958-0, pp. 141-146.

Singer, N.C., Seering, W.P. (1990) Preshaping command inputs to reduce system vibration, Trans. ASME, J. Dyn. Syst. Meas. Control, vol. 112, no. 1, pp. 76–82.

Singh, T., Singhose, W. (2002) Input shaping/time delay control of maneuvering flexible structures, In: Proceedings of the 2002 American Control Conference, 2002, Vol. 3, pp. 1717-1731.

Varghese, M., Amantea, R., Sauer, D., Senturia, S.D. (1997) Resistive damping of pulse-sensed capacitive position sensors, In: Proceedings of the International Conference on Solid State Sensors and Actuators, TRANSDUCERS '97 Chicago, Vol. 2, pp. 1121-1124.

Thielemann, J., Sandner, T., Schwarzer, S., Cupcic, U., Schumann-Olsen, H., Kirkhus, T. (2010) TACO: Three-dimensional Camera with Object Detection and Foveation, *EC FP7 grant no 248623*, http://www.taco-project.eu/

Zeitz, M. (2012) Feedforward Control Design in the Frequency Domain: Offline or Online (in German), Automatisierungstechnik 60 (2012), pp. 375-383.

Zhu, G., Levine, J., Praly, L., Peter, Y.-A. (2006) Flatness-Based Control of Electrostatically Actuated MEMS With Application to Adaptive Optics: A Simulation Study, Journal of Microelectromechanical Systems, Vol. 15 , Issue 5, pp. 1165-1174.

Post-print version of the article: K. Janschek, T. Sandner, R. Schroedter, M. Roth, "Adaptive Prefilter Design for Control of Quasistatic Microscanners", *Proc. of 6th IFAC Symposium on Mechatronic Systems*, vol. 46 (5), pp. 197-206, 2013.
DOI: 10.3182/20130410-3-CN-2034.00112

For further information contact: schroedter@acin.tuwien.ac.at, https://orcid.org/0000-0003-3259-4571

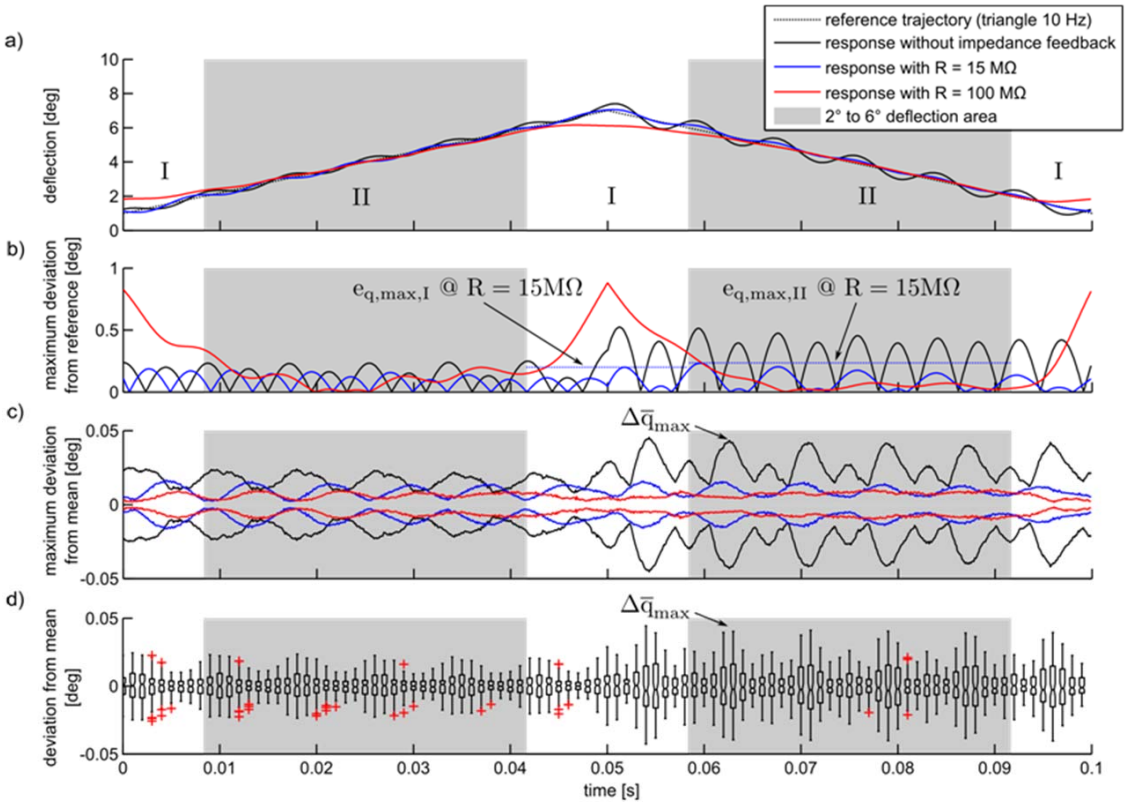

Fig. 17. Experimental results for characteristic triangular reference deflection commands with different impedance feedback (configuration: static prefilter only): a) typical instantaneous mirror deflection, b) maximum deviation $e_{q,\max}$ from reference mirror deflection, c) deviation $\triangle\overline{q}(t_i)$ from mean mirror deflection for 99 periods, d) boxplot[1] of deviation $\triangle\overline{q}(t_i)$ from mean mirror deflection for response without impedance feedback

[1]boxplot: The box contents 50 percent of the data within the upper and lower quartile and is notched at median. Whiskers are connecting the box to the 1.5 interquartile range (IQR) of upper and lower quartile. The outliers are illustrated with red crosses. (cf. MATLAB Boxplot http://www.mathworks.de/de/help/stats/boxplot.html)

Post-print version of the article: K. Janschek, T. Sandner, R. Schroedter, M. Roth, "Adaptive Prefilter Design for Control of Quasistatic Microscanners", *Proc. of 6th IFAC Symposium on Mechatronic Systems*, vol. 46 (5), pp. 197-206, 2013.
DOI: 10.3182/20130410-3-CN-2034.00112

For further information contact: schroedter@acin.tuwien.ac.at, https://orcid.org/0000-0003-3259-4571